CrossMark
click for updates

Biochar-supported carbon nanotube and graphene oxide nanocomposites for Pb(II) and Cd(II) removal

Taoze Liu,[ab] Bin Gao,[*b] June Fang,[b] Bing Wang[a] and Xinde Cao[c]

Carbon materials such as nanoparticles have provided new solutions for the removal of various environmental contaminants. In this work, two carbon nanomaterial–biochar nanocomposites (SG–PySA–CNT and SG–PySA–GO) were derived from sweetgum biomass pretreated with carbon nanotubes (CNTs) and graphene oxide (GO) through slow pyrolysis at 600 °C. Both SG–PySA–CNT and SG–PySA–GO had higher surface area but much lower pore volume than the pristine biochar (SG). Batch sorption experimental results showed that SG–PySA–CNT and SG–PySA–GO had greater sorption ability to Pb(II) and Cd(II) from aqueous solution than SG. SG–PySA–GO was the best sorbent with maximum sorption capacities higher than 40 and 10 mg g^{-1} for Pb(II) and Cd(II), respectively. The enhanced metal sorption by the biochar nanocomposites could be mainly attributed to the excellent sorptive properties of the carbon nanoparticles (CNT/GO) distributed and stabilized on the biochar surfaces within the matrix. Because of its facile synthesis and good sorptive properties, biochar-supported CNT and GO nanocomposites have great potential to be used in various environmental applications for the removal of metal and metalloid contaminants.

1. Introduction

With the rapid development of industries such as mining operations, metal processing plants, fertilizer manufacturers, *etc.*, metal and metalloid pollutants have increasingly been directly or indirectly released into natural water bodies.[1] Because of their high solubility in aquatic environments, metal and metalloid ions are not biodegradable and tend to be accumulated by living organisms, which causes serious toxic effects to the ecosystems and public health.[2,3] Many methods thus have been developed for efficient metal and metalloid

removal from wastewater such as chemical precipitation, sorption, membrane filtration, and electrochemical technologies.[4,5] Among these methods, sorption is known for its ease of operation and low maintenance cost; therefore, research on high efficiency, low-cost sorbents for heavy metals has attracted considerable attention.[6]

Biochar, a porous carbon material, has been proposed by many researchers as an alternative, low-cost sorbent for environmental remediation, particularly for the removal of heavy metals from aqueous solutions.[5,7] Furthermore, recent studies have suggested that combining traditional biochar technology with other emerging technologies, such as biotechnology and nanotechnology, can create "engineered biochars" or "designer biochars" with unique physicochemical characteristics and enhanced sorptive abilities for the removal of heavy metals and other contaminants.[8–10]

In addition to low-cost, bulk carbon materials, carbon-based nanomaterials such as graphene (GR) and carbon nanotubes (CNT) of various forms have also shown great binding affinity to metal and metalloid ions in aqueous solutions.[11,12] GR and CNT can be functionalized with –OH and –COOH groups *via* chemical oxidation methods,[13] which may increase their sorption ability to metal and metalloid ions due to the strong complexation between the metal ions and the functional groups.[14] The direct applications of carbon nanomaterials to remove aqueous contaminants, however, are limited due to the concerns over nanoparticle elution from the system.[12,15] Novel techniques thus have been developed to stabilize carbon nanomaterials in nanocomposites or gels to promote their applications as sorbents for the removal of aqueous contaminants.[16,17] Several recent studies have shown that biochar, because of its porous structure and relatively high surface area, can be used as a host to distribute and stabilize carbon nanomaterials such as GR and CNT.[17–19] Because both the biochar matrix and the stabilized carbon nanomaterials have good sorptive properties, the biochar-based nanocomposites are promising sorbents for contaminants, particularly metals and metalloids in aqueous solutions.

[a]State Key Laboratory of Environmental Geochemistry, Institute of Geochemistry, Chinese Academy of Sciences, Guiyang 550002, China

[b]Department of Agricultural and Biological Engineering, University of Florida, Gainesville, FL 32611, USA. E-mail: bg55@ufl.edu; Fax: +1 352 392 4092; Tel: +1 352 392 1864 extn 285

[c]School of Environmental Science and Engineering, Shanghai Jiaotong University, Shanghai 200240, China

The objective of this work was to further evaluate the potentials of carbon nanomaterials–biochar nanocomposites as effective sorbents to remove heavy metals from aqueous solutions. Two types of biochar-based nanocomposites were produced in laboratory through slow pyrolysis of sweetgum (*Liquidambar styraciflua*) pre-treated with CNT and graphene oxide (GO). Laboratory batch sorption experiments were then carried out to examine and compare the sorption characteristics of Pb(II) and Cd(II) onto the biochar sorbents. Mathematical models and characterization tools were used to help explore the sorption mechanisms.

2. Materials and methods

2.1. Materials

Sweetgum wood was collected locally (Gainesville, FL) and ground in a knife mill to a size of 0.5–1 mm as the feedstock for biochar production. Two types of carbon nanomaterials: multiwalled CNT (Sinonano, Nanjing, China) with diameters of 10–20 nm and GO (ACS Material, Medford, MA) with thickness of 0.8–1.2 nm were used as received. Lead nitrate, cadmium nitrate, and 1,3,6,8-pyrenetetrasulfonic acid tetrasodium salt hydrate (PySA) were obtained from Sigma-Aldrich and used as received.

2.2. Preparation of the sorbents

The method of preparing carbon nanomaterial–biochar nanocomposites was modified from previous studies.[18,19] A carbon nanomaterial suspension was first prepared by adding 0.2 g of CNT or GO and 0.4 g of PySA powder, into 200 mL of deionized (DI) water. The suspension was then stirred and sonicated for 1 h in an ultrasonicator (3510R-DTH, Bransonic Ultrasonics Corporation). The resulting suspension was used to prepare the biochar-based nanocomposites. About 20 g of the sweetgum feedstock were thoroughly dip-coated with the suspension for 2 h and was then oven-dried at 70 °C. The carbon nanomaterials-treated feedstock were placed inside a tube furnace (MTI, Richmond, CA) to produce the nanocomposites through slow pyrolysis at 600 °C for 1 h in a N_2 environment. Feedstock without carbon nanomaterials was also used to produce pristine biochar under the same pyrolysis conditions (*i.e.*, 600 °C for 1 h in a N_2 environment). The pristine biochar and two carbon nanomaterial–biochar nanocomposites were designated as SG, SG–PySA–CNT, and SG–PySA–GO, respectively. The biochar sorbents were washed with DI water for several times to remove potential impurities, oven dried, and sealed in containers before further testing.

2.3. Characterizations

Contents of carbon (C), hydrogen (H) and nitrogen (N) in the samples were determined using a CHN Elemental Analyzer (Carlo Erba NA-1500) *via* high-temperature catalyzed combustion followed by infrared detection of the resulting CO_2, H_2 and NO_2 gases, respectively. Specific surface area of biochars was measured using N_2 sorption on a NOVA 1200 analyzer and calculated using Brunauer–Emmett–Teller (BET) method. Thermogravimetric analysis (TGA) of the samples was performed in a stream of air at a heating rate of 10 °C min^{-1} with a Mettler TGA analyzer (Columbus, OH).

2.4. Sorption of lead and cadmium

Heavy metal solutions were prepared by dissolving lead nitrate and cadmium nitrate in DI water. Sorption kinetics of Pb(II) and Cd(II) on each biochar sample were examined by mixing 0.05 g of the sorbent with 50 mL of Pb(II) (100 mg L^{-1}) or Cd(II) (50 mg L^{-1}) solutions in 68 mL digestion vessels (Environmental Express) at room temperature (22 ± 0.5 °C). The vessels were shaken on a mechanical shaker at 50 rpm until sampling. At each sampling time (0.5, 1, 2, 4, 8, 12, 24, and 48 h), the suspensions were immediately filtered through 0.22 μm pore size nylon membrane filters (GE cellulose nylon membrane). Concentrations of Pb(II) and Cd(II) in the filtrates were determined with an inductively coupled plasma-atomic emission spectrometry (ICP-AES, Perkin-Elmer Plasma 3200). Sorption isotherms were determined by mixing 0.05 g of each biochar with 50 mL of varying concentration Pb(II) (30–200 mg L^{-1}) or Cd(II) (20–150 mg L^{-1}). The suspension was shaken on the shaker at room temperature for 24 h, and then treated as described above. All the sorption experiments were conducted in duplicate, and the average experimental data was reported. Various models were used to simulate the sorption kinetics and isotherms.

3. Results and discussion

3.1. Biochar properties

The physico-chemical characteristics of the pristine biochar and two biochar-based nanocomposites are shown in Table 1. Specific surface area and pore volume of the pristine biochar were 234.1 m^2 g^{-1} and 0.034 cm^3 g^{-1}, respectively. SG–PySA–CNT and SG–PySA–GO showed significant increase in the specific surface area (292.5 m^2 g^{-1} and 369.9 m^2 g^{-1}, respectively), but their pore volume values were much lower (<0.001 cm^3 g^{-1}) than that of the pristine biochar. These changes reflected that the carbon nanomaterials might be stabilized on the biochar surfaces within the pore networks, which could increase the surface, but at the same time, might block the pores or pore-openings of the biochars. CHN analysis indicated that the pristine biochar and the engineered biochars were all carbon-rich with carbon compositions ranging 78.6–81.9% (Table 1), which is typical of pyrolyzed biomass.[17,20] The nitrogen and hydrogen contents of the tested biochars were similar and ranged from 0.34–0.58% and 2.38–3.15%, respectively (Table 1).

TGA profiles (Fig. 1) showed that the pristine and engineered biochars had negligible weight losses when temperature was less than 380 °C, indicating all of them were well-carbonized with good thermal stability. In comparison to pristine biochar, the SG–PySA–CNT and SG–PySA–GO showed slightly higher heat resistance when the temperature was higher. This could be attributed to the good thermal stability of CNT and GO on the biochar surfaces that improve their anti-thermal decomposition abilities.[17,18]

Table 1 Basic physiochemical properties of biochar samples[a]

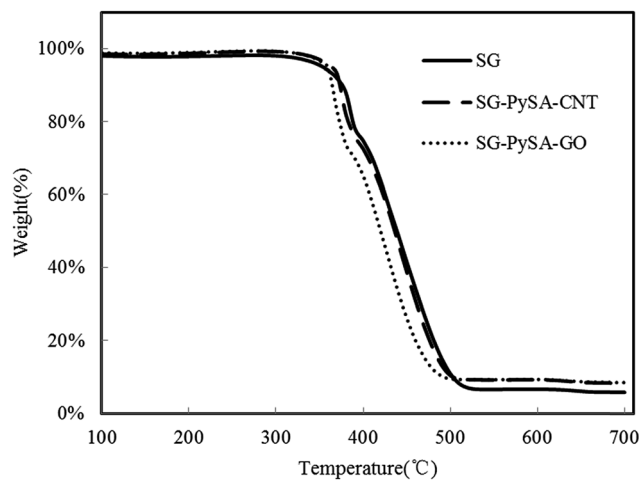| Sample	Surface area ($m^2\ g^{-1}$)	Pore volume ($cm^3\ g^{-1}$)	C%	N%	H%
SG	234.1	0.034	81.9	0.34	2.38
SG–PySA–CNT	292.5	0.001	79.1	0.58	3.15
SG–PySA–GO	369.9	—	78.6	0.35	2.46

[a] "—": <0.001.

Fig. 1 TGA profiles of the biochar samples.

3.2. Sorption kinetics

Sorption kinetics of the two heavy metals to the three biochars showed similar trends (Fig. 2). However, the GO- and CNT-biochars sorbed more Pb(II) and Cd(II) than the pristine biochar, indicating the carbon nanomaterials on the biochar surface could serve as active sorption sites for the heavy metals. Several previous studies have demonstrated that both GO and CNT have strong sorption abilities to various contaminants including Pb(II) and Cd(II).[11,12,21] Mathematical models were applied to simulate the experimental kinetics (Table 2). Besides commonly used pseudo-first-order and pseudo-second-order models, the Ritchie n_th-order and the Elovich models were also included[22]

$$\frac{dq_t}{dt} = k_1(q_e - q_t), \text{ first-order} \tag{1}$$

$$\frac{dq_t}{dt} = k_2(q_e - q_t)^2, \text{ second-order} \tag{2}$$

$$\frac{dq_t}{dt} = k_n(q_e - q_t)^n, \text{ Ritchie } n\text{_th-order} \tag{3}$$

$$\frac{dq_t}{dt} = \alpha \exp(-\beta q_t), \text{ Elovich} \tag{4}$$

where q_t (mg g^{-1}) and q_e (mg g^{-1}) are the amount of Pb(II) and Cd(II) sorbed at time t and at equilibrium, respectively; k_1 (h^{-1}), k_2 (g mg^{-1} h^{-1}), and k_n (g^{n-1} mg^{1-n} h^{-1}) are the first-order, second-order, and Ritchie n_th-order sorption rate constants;
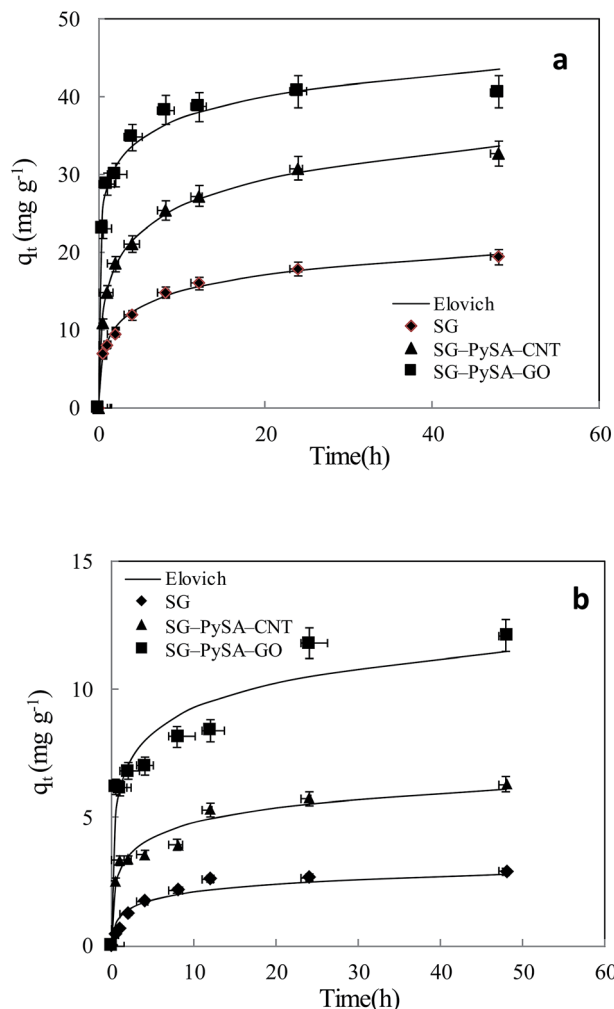

Fig. 2 Sorption kinetics of Pb(II) (a) and Cd(II) (b) onto biochar samples. Symbols are experimental data and lines are model results.

α (mg g^{-1} h^{-1}) is the initial sorption rate; and β (g mg^{-1}) is the desorption constant. The first-order, second-order, and Ritchie models describe the kinetics of the solid-solution system based on mononuclear, binuclear, and n-nuclear sorption, respectively, with respect to the sorbent capacity, and the Elovich model is an empirical equation considering the contribution of desorption.[22] Among all the tested models, the Elovich and Ritchie models described the Pb(II) and Cd(II) sorption kinetics better than the other models (Table 2). The model results suggested that the sorption of Pb(II) and Cd(II) onto the biochar samples might be controlled by multiple interaction mechanisms or processes. Previous studies have demonstrated that both biochar matrix and the carbon nanoparticles of the nanocomposites contribute to the sorption of heavy metals form aqueous solution, which may complicate the sorption process and mechanisms.[19] In addition, the sorption of heavy metals such as Pb(II) and Cd(II) onto pristine biochar is controlled by multiple mechanisms such as precipitation, complexation, electrostatic attraction, surface adsorption, etc.[5]

Table 2 Summary best-fit parameters of various kinetic models

Sorbents	Model	Sorbate	Parameter 1	Parameter 2	Parameter 3	R^2
SG	Elovich	Pb(II)	$\alpha = 42.9$	$\beta = 0.330$		0.990
	1st order		$k = 0.473$	$q_e = 16.9$		0.792
	2nd order		$k = 0.0350$	$q_e = 18.6$		0.920
	Ritchie		$k = 0.0000300$	$q_e = 26.5$	$n = 4.98$	0.978
SG–PySA–CNT	Elovich		$\alpha = 93.0$	$\beta = 0.202$		0.994
	1st order		$k = 0.590$	$q_e = 28.3$		0.819
	2nd order		$k = 0.0250$	$q_e = 31.2$		0.944
	Ritchie		$k = 0.0000400$	$q_e = 41.3$	$n = 4.36$	0.994
SG–PySA–GO	Elovich		$\alpha = 4460$	$\beta = 0.250$		0.931
	1st order		$k = 1.49$	$q_e = 37.8$		0.760
	2nd order		$k = 0.0580$	$q_e = 40.1$		0.946
	Ritchie		$k = 0.00200$	$q_e = 44.7$	$n = 3.37$	0.980
SG	Elovich	Cd(II)	$\alpha = 4.79$	$\beta = 2.24$		0.895
	1st order		$k = 0.255$	$q_e = 2.70$		0.983
	2nd order		$k = 0.100$	$q_e = 3.10$		0.993
	Ritchie		$k = 0.0650$	$q_e = 2.95$	$n = 1.66$	0.994
SG–PySA–CNT	Elovich		$\alpha = 26.4$	$\beta = 1.20$		0.913
	1st order		$k = 0.859$	$q_e = 5.00$		0.500
	2nd order		$k = 0.180$	$q_e = 5.60$		0.720
	Ritchie		$k = 0.0000100$	$q_e = 9.89$	$n = 7.65$	0.881
SG–PySA–GO	Elovich		$\alpha = 103$	$\beta = 0.711$		0.845
	1st order		$k = 1.27$	$q_e = 9.3$		0.300
	2nd order		$k = 0.143$	$q_e = 10.3$		0.550
	Ritchie		$k = 8.50$	$q_e = 16.2$	$n = 6.77$	0.780

3.3. Sorption isotherm

The sorption isotherms of Pb(II) and Cd(II) onto the biochar samples showed the sorption capacities of the sorbents followed the order of SG–PySA–GO > SG–PySA–CNT > SG (Fig. 3). The metal sorption capacities of the biochar nanocomposites were much higher than that of the pristine biochar, confirming that the GO and CNT particles contributed greatly to the sorption ability of the sorbents. Previous studies have shown that GO may have much higher sorption capacities than CNT to heavy metal ions in aqueous solutions,[23] which may explain why SG–PySA–GO had higher sorption capacities to Pb(II) and Cd(II) than SG–PySA–CNT in this work. The maximum Pb(II) and Cd(II) sorption capacities of the SG–PySA–GO were the highest with values greater than 40 and 10 mg g^{-1}, respectively (Fig. 3). Four commonly used isotherm equations were used to simulate the experimental isotherms (Table 3), and the governing equations can be written as:[22,24]

$$q_e = \frac{KQC_e}{1 + KC_e}, \text{ Langmuir} \tag{5}$$

$$q_e = K_f C_e{}^n, \text{ Freundlich} \tag{6}$$

$$q_e = \frac{RT}{b} \ln(AC_e), \text{ Temkin} \tag{7}$$

$$\ln q_e = \ln q_{max} - K_d \varepsilon^2, \text{ Dubinnin–R} \tag{8}$$

where K (L mg^{-1}), K_f (mg$^{(1-n)}$ L^n g^{-1}), and K_d (mg^2 J^{-2}) represent the Langmuir bonding term related to interaction energies, the
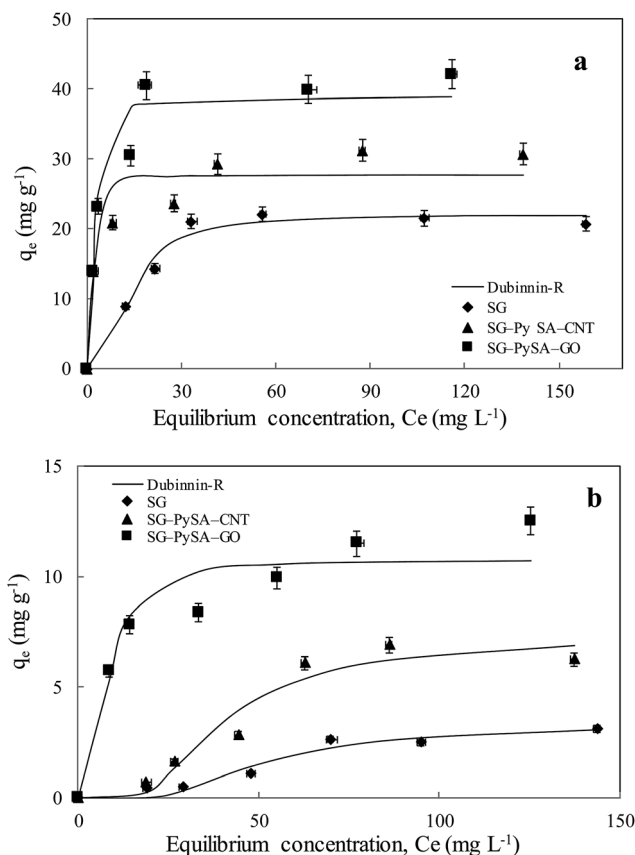

Fig. 3 Sorption isotherms of Pb(II) (a) and Cd(II) (b) onto biochar samples. Symbols are experimental data and lines are model results.

Table 3 Summary of best-fit parameters of various isotherm models

Sorbents	Model	Sorbate	Parameter 1	Parameter 2	R^2
SG	Langmuir	Pb(II)	$K = 0.072$	$S_{max} = 24.9$	0.788
	Freundlich		$K = 7.78$	$n = 0.217$	0.582
	Temkin		$K_t = 1.31$	$S_{max} = 4.44$	0.657
	Dubinnin–R		$K_d = 174.49$	$S_{max} = 22.3$	0.976
SG–PySA–CNT	Langmuir		$K = 0.331$	$S_{max} = 30.4$	0.895
	Freundlich		$K = 13.87$	$n = 0.174$	0.924
	Temkin		$K_t = 15.65$	$S_{max} = 4.19$	0.951
	Dubinnin–R		$K_d = 4.53$	$S_{max} = 27.68$	0.913
SG–PySA–GO	Langmuir		$K = 0.277$	$S_{max} = 43.2$	0.940
	Freundlich		$K = 17.93$	$n = 0.194$	0.798
	Temkin		$K_t = 7.69$	$S_{max} = 6.60$	0.866
	Dubinnin–R		$K_d = 7.12$	$S_{max} = 38.6$	0.950
SG	Langmuir	Cd(II)	$K = 0.002$	$S_{max} = 99.4$	0.848
	Freundlich		$K = 0.05$	$n = 0.833$	0.864
	Temkin		$K_t = 0.06$	$S_{max} = 1.48$	0.902
	Dubinnin–R		$K_d = 2036.24$	$S_{max} = 3.39$	0.941
SG–PySA–CNT	Langmuir		$K = 0.008$	$S_{max} = 14.1$	0.799
	Freundlich		$K = 0.25$	$n = 0.695$	0.746
	Temkin		$K_t = 0.07$	$S_{max} = 3.35$	0.865
	Dubinnin–R		$K_d = 1250.6$	$S_{max} = 7.36$	0.943
SG–PySA–GO	Langmuir		$K = 0.09$	$S_{max} = 12.7$	0.907
	Freundlich		$K = 3.53$	$n = 0.262$	0.957
	Temkin		$K_t = 1.47$	$S_{max} = 2.34$	0.954
	Dubinnin–R		$K_d = 58.58$	$S_{max} = 10.8$	0.928

Freundlich affinity coefficient, and DR constant of sorption energy, respectively; Q (mg g^{-1}) denotes the Langmuir maximum capacity; C_e (mg L^{-1}) is the equilibrium solution concentration of the sorbate; n (dimensionless) is the Freundlich linearity constant; b (J g mg^{-1}) and A (L mg^{-1}) are the Temkin isotherm constants; and ε is the Polanyi potential. The Pb(II) and Cd(II) sorption isotherms were better fitted with the Dubinnin–R model than the others and the R^2 values were more than 0.9 (Table 3), suggesting that the interactions between the two heavy metals and the biochar sorbents might be mainly controlled by the Dubinnin–R processes. The Dubinnin–R isotherm describes the sorption on a single type of uniform pores and is applied to distinguish between physical and chemical sorption, which does not assume a homogeneous surface or a constant sorption potential.[18] The Dubinnin–R maximum sorption capacities of SG–PySA–GO to Pb(II) and Cd(II) were 38.6 and 10.8 mg g^{-1}, respectively, which are much higher than that of SG (22.2 and 3.4 mg g^{-1}). This further confirmed that the presence of carbon nanomaterials significantly increased heavy metals sorption ability of the engineered biochars.

3.4. Sorption mechanisms

Findings form this work indicated that incorporation of carbon nanomaterials (CNT and GO) into biochar effectively enhanced its sorption of Pb(II) and Cd(II) in aqueous solutions. In comparison to the pristine biochar, the sorption capacities of the SG–PySA–CNT and SG–PySA–GO nanocomposites increased 0.5–1.0 and 2.0–5.0 times for Pb(II) and Cd(II), respectively. Likewise, previous studies have suggested that other conventional absorbents such as sand coated carbon nano-materials can exhibit better removal ability of heavy metals.[12,25] Possible mechanisms of the removal of Pb(II) and Cd(II) by the biochar nanocomposites include: complexation with oxygen containing functional groups of the carbon nanomaterials, cation exchange by exchangeable sites on the biochar surfaces, electrostatic attraction, and surface adsorption onto both the carbon nanomaterial and biochar surfaces.[17,26] Several of previous studies have demonstrated that the carboxyl (–COOH) and hydroxyl (–OH) of both GO and functionalized CNTs can form strong complexes with Pb(II) and Cd(II) in aqueous solutions.[23,27] In addition, the basal planes of the GO may attraction metal ions including Pb(II) and Cd(II) through pi-interactions,[23] which is consistent with the experimental results that SG–PySA–GO showed higher sorption ability to the two heavy metals than SG–PySA–CNT.

4. Conclusions

Biochar-based CNT and GO nanocomposites were prepared by direct pyrolysis of biomass pretreated with corresponding carbon nanomaterials. As porous materials, the biochar provided both pore space and surface sites to distribute and stabilize the carbon nanomaterials to form nanocomposites. Compared to the pristine biochar, the two biochar-based nanocomposites showed improved special surface area and enhanced sorption ability to aqueous Pb(II) and Cd(II). Because of the excellent sorption ability of the carbon nanomaterials, especially GO, to the metal and metalloid ions, the biochar-based nanocomposites showed great potential to be used as

an effective sorbent for the treatment and remediation of metal and metalloid contaminants.

Acknowledgements

References

1 V. K. Gupta, O. Moradi, I. Tyagi, S. Agarwal, H. Sadegh, R. Shahryari-Ghoshekandi, A. S. H. Makhlouf, M. Goodarzi and A. Garshasbi, *Crit. Rev. Environ. Sci. Technol.*, 2016, **46**, 93–118.

2 N. Gupta, D. K. Khan and S. C. Santra, *Environ. Monit. Assess.*, 2012, **184**, 6673–6682.

3 G. H. Kumar and J. P. Kumari, *Water, Air, Soil Pollut.*, 2015, **226**, 324.

4 F. Fu and Q. Wang, *J. Environ. Manage.*, 2011, **92**, 407–418.

5 M. Inyang, B. Gao, Y. Yao, Y. Xue, A. Zimmerman, A. Mosa, P. Pullammanappallil, Y. Ok and X. Cao, *Crit. Rev. Environ. Sci. Technol.*, 2016, **46**, 406–433.

6 D. Kailash, P. Dharmendra and V. Anil, *Res. J. Chem. Environ.*, 2010, **14**, 100–103.

7 D. Mohan, A. Sarswat, Y. S. Ok and C. U. Pittman Jr, *Bioresour. Technol.*, 2014, **160**, 191–202.

8 Y. S. Ok, S. X. Chang, B. Gao and H.-J. Chung, *Environmental Technology & Innovation*, 2015, **4**, 206–209.

9 M. Inyang, B. Gao, Y. Yao, Y. Xue, A. R. Zimmerman, P. Pullammanappallil and X. Cao, *Bioresour. Technol.*, 2012, **110**, 50–56.

10 M. Zhang and B. Gao, *Chem. Eng. J.*, 2013, **226**, 286–292.

11 Z. H. Ding, X. Hu, V. L. Morales and B. Gao, *Chem. Eng. J.*, 2014, **257**, 248–252.

12 Y. Tian, B. Gao, V. L. Morales, L. Wu, Y. Wang, R. Munoz-Carpena, C. Cao, Q. Huang and L. Yang, *Chem. Eng. J.*, 2012, **210**, 557–563.

13 V. Datsyuk, M. Kalyva, K. Papagelis, J. Parthenios, D. Tasis, A. Siokou, I. Kallitsis and C. Galiotis, *Carbon*, 2008, **46**, 833–840.

14 P. O. Boamah, Y. Huang, M. Q. Hua, Q. Zhang, J. B. Wu, J. Onumah, L. K. Sam-Amoah and P. O. Boamah, *Ecotoxicol. Environ. Saf.*, 2015, **116**, 113–120.

15 Y. Tian, B. Gao, V. L. Morales, H. Chen, Y. Wang and H. Li, *Chemosphere*, 2013, **90**, 2597–2605.

16 M. Zhang, B. Gao, X. D. Cao and L. Y. Yang, *RSC Adv.*, 2013, **3**, 21099–21105.

17 M. Inyang, B. Gao, A. Zimmerman, M. Zhang and H. Chen, *Chem. Eng. J.*, 2014, **236**, 39–46.

18 M. Zhang, B. Gao, Y. Yao, Y. W. Xue and M. Inyang, *Sci. Total Environ.*, 2012, **435**, 567–572.

19 M. Inyang, B. Gao, A. Zimmerman, Y. M. Zhou and X. D. Cao, *Environ. Sci. Pollut. Res.*, 2015, **22**, 1868–1876.

20 J. Tang, W. Zhu, R. Kookana and A. Katayama, *J. Biosci. Bioeng.*, 2013, **116**, 653–659.

21 M. Kılıç, Ç. Kırbıyık, Ö. Çepelioğullar and A. E. Pütün, *Appl. Surf. Sci.*, 2013, **283**, 856–862.

22 Y. Yao, B. Gao, M. Inyang, A. R. Zimmerman, X. D. Cao, P. Pullammanappallil and L. Y. Yang, *J. Hazard. Mater.*, 2011, **190**, 501–507.

23 G. Zhao, J. Li, X. Ren, C. Chen and X. Wang, *Environ. Sci. Technol.*, 2011, **45**, 10454–10462.

24 P. D. Bhalara, D. Punetha and K. Balasubramanian, *Int. J. Environ. Sci. Technol.*, 2015, **12**, 3095–3106.

25 W. Gao, M. Majumder, L. B. Alemany, T. N. Narayanan, M. A. Ibarra, B. K. Pradhan and P. M. Ajayan, *ACS Appl. Mater. Interfaces*, 2011, **3**, 1821–1826.

26 V. K. Gupta, S. Agarwal and T. A. Saleh, *J. Hazard. Mater.*, 2011, **185**, 17–23.

27 G. P. Rao, C. Lu and F. Su, *Sep. Purif. Technol.*, 2007, **58**, 224–231.